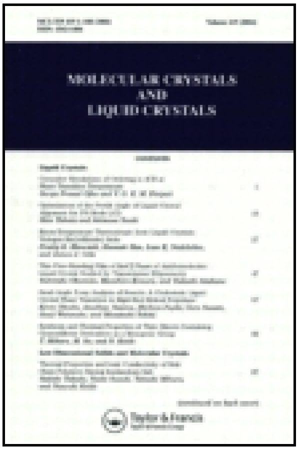

Molecular Crystals and Liquid Crystals
Publication details, including instructions for authors and subscription information:
http://www.tandfonline.com/loi/gmcl18

Defect Dynamics and Statistics of Defect Chaos in Electrohydrodynamic Convections in Nematics

S. Kai [a] , M. Kohno [a] , M. Andoh [a] , M. Imasaki [a] & W. Zimmermann [b]
[a] Department of Electrical Engineering, Kyushu Institute of Technology, Tobata, Kirakyushu, 804, Japan
[b] IFF Theorie ill, Forschungszentrurn Juelich KFA, D-5170, Juelich, FRG
Version of record first published: 24 Sep 2006.

Mol. Cryst. Liq. Cryst., 1991, Vol. 198, pp. 247–253
Reprints available directly from the publisher
Photocopying permitted by license only

Printed in the United States of America

Defect Dynamics and Statistics of Defect Chaos in Electrohydrodynamic Convections in Nematics

S. KAI, M. KOHNO, M. ANDOH and M. IMASAKI

Department of Electrical Engineering, Kyushu Institute of Technology, Tobata, Kitakyushu 804, Japan

and

W. ZIMMERMANN†

†IFF Theorie III, Forschungszentrum Juelich KFA, D-5170, Juelich FRG

(Received July 25, 1990)

Defect dynamics and chaos in electrohydrodynamic convections of nematic liquid crystals, which appear in the state slightly above the Williams domain convection (WD) occurring at a threshold voltage V_c, are statistically investigated. The temporal change and ε-dependence of mean defect number are measured for two different aspect ratios Γ (ratio of the lateral dimension to the thickness of the layer) = 15 and 650 in the conduction regime, where $\varepsilon = (V^2 - V_c^2)/V_c^2$. The power spectrum for the temporal change of the defect number is calculated. For small $\Gamma = 15$ the spectrum shows $1/f$-type independently of ε. For large $\Gamma = 650$ defect turbulence called the fluctuating WD, appears at a voltage very close to V_c. The spectrum shows white at relatively large ε and $1/f$ spectrum at very small ε. The probability distributions of defect numbers are rather well-fitted with Poisson distribution. The ε-dependence of mean defect number in the distribution clearly changes at identical ε where spectrum profile changes from $1/f$ to white. In the region indicating $1/f$ spectrum, the mean defect number is approximately proportional to ε^2 whereas in the region with white spectrum, i.e. large ε, it is proportional to $\varepsilon^{0.95}$. This cross-over is only observed in the cell with $\Gamma = 650$. But no change of the dependence is observed for $\Gamma = 15$. This probably suggests the possibility of two different dynamics for defect turbulence.

Keywords: electrohydrodynamic convections, nematics, defect chaos

1. INTRODUCTION

Occurrence of defect turbulence is one of mysterious phenomena.[1–3] Questions why and how topological defects continuously nucleate and annihilate, and how realize defect turbulence are not yet fully understood at all. Investigations for statistical properties on these subjects have been achieved recently experimentally and theoretically.[4–9] Very recently Gil, Lega and Meunier suggest that the distribution will be given by square Poisson consisting of the Bessel function under assumption with independent nucleation and annihilation of defect pairs.[7] Furthermore they give a qualitative interpretation for occurrence of defect-mediated turbulence from a viewpoint of phase instabilities. Then an experimental investigation reported well-fitted results with their theory.[4] However they are not sufficiently successful and quantitative. Now many researchers pay great attention to the mechanism of defect-mediated turbulence.[4–10]

In this article we will report some details of statistical properties not only distributions of defect numbers but also the power spectrum of nonperiodic change of defect numbers and those dependent on external control parameters, i.e. voltage and aspect ratio. We investigate here a temporal nonperiodic change of defect numbers in electrohydrodynamic convections (EHDC) and try to fit it with both Poisson and square Poisson distributions. We have done these experiments in fluctuating Williams domain (FWD) regime in EHDC in nematic liquid crystals. The experimental set-up is standard one and already reported elsewhere.[5] Five sample cells with two different aspect ratios were prepared.

2. EXPERIMENTAL

Figure 1 shows spatio-temporal patterns of FWD, where ε is a normalized voltage as $(V^2 - V_c^2)/V_c^2$ by the threshold V_c of the WD instability, for $\Gamma = 15$ and 650 respectively. Here x is in the direction parallel to an original director orientation. Eventually both spatio-temporal patterns are quite different from each other. For $\Gamma = 15$, first, a threshold $V_c^* = 8.80$ V (corresponding normalized parameter $\varepsilon_c^* = 0.43$) for the onset of FWD is higher than that ($\varepsilon_c^* = 7.80$ V and $\varepsilon_c^* = 0.24$) for $\Gamma = 650$. Namely the larger the Γ, the easier the formation of FWD. Secondly, in the smaller aspect ratio $\Gamma = 15$, long spatial coherency of defect motions can be observed perpendicular to the roll axis (indicated as bright horizontal lines), but not in the larger one. The gliding motion in FWD in a small aspect ratio is rather coherent. These suggest the strong boundary effects (Γ effects on kinetics of FWD).

Figures 2 and 3 show $\varepsilon-$ dependences of correlation lengths and times for both Γs obtained from spatio-temporal maps as shown in Figure 1. The relations are respectively given by the equations,

$$\xi/d = \xi_{10}(\varepsilon - \varepsilon_c^*)^{-0.135} \tag{1}$$

$$\tau = \tau_{10}(\varepsilon - \varepsilon_c^*)^{-0.113} \tag{2}$$

for $\Gamma = 15$, and for 650,

$$\xi/d = \xi_{20}(\varepsilon - \varepsilon_c^*)^{-0.516} \tag{3}$$

$$\tau = \tau_{20}(\varepsilon - \varepsilon_c^*)^{-0.529}, \tag{4}$$

where $\xi_{10} = 1.03$, $\tau_{10} = 60.3$ s, $\xi_{20} = 0.66$, and $\tau_{20} = 11.4$ s. Here d is the thickness

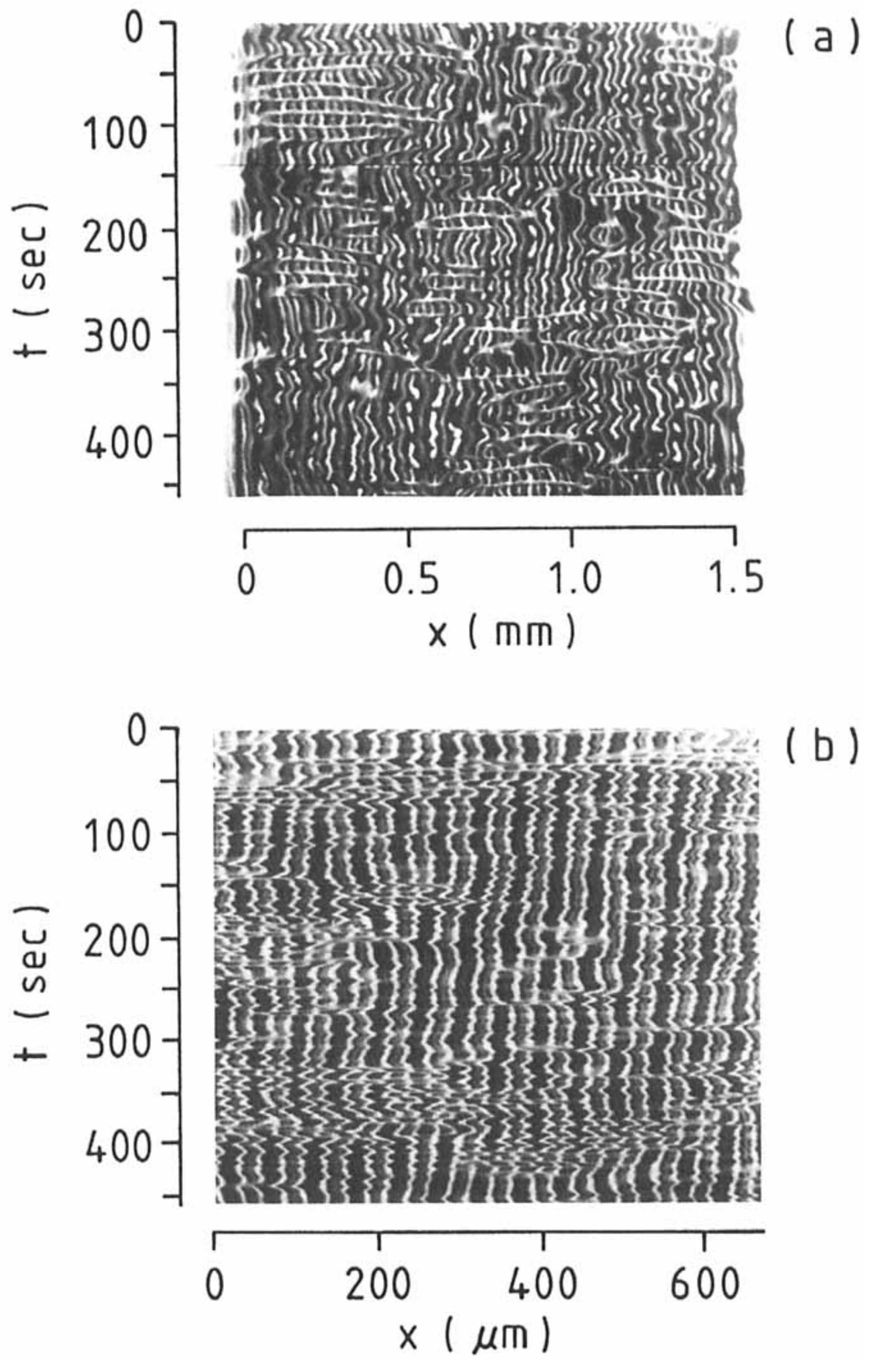

FIGURE 1 Spatio-temporal patterns of FWD. (a) For $\Gamma = 15$ (sample No. 1: 1.5 × 1.0 mm, d = 100 μm, f = 20 Hz, V_c = 7.37 V, f_c = 62 Hz, V_c^* = 8.80 V, ε_c^* = 0.43) ε = 1.65 (b) $\Gamma = 650$ (sample No. 2: 3.0 × 3.0 cm, d = 46 μm, f = 20 Hz, V_c = 7.00 V, f_c = 90 Hz, V_c^* = 7.80 V, ε_c^* = 0.24) ε = 0.73. The pattern is taken just center of the whole cell for $\Gamma = 650$.

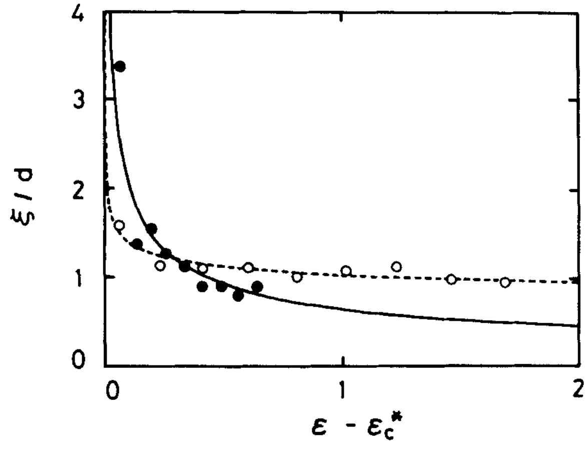

FIGURE 2 ε dependence of normalized correlation length ξ/d calculated from spatio-temporal maps. The closed and open circles show the results for $\Gamma = 650$ and 15, respectively. The line is obtained by the least mean square method.

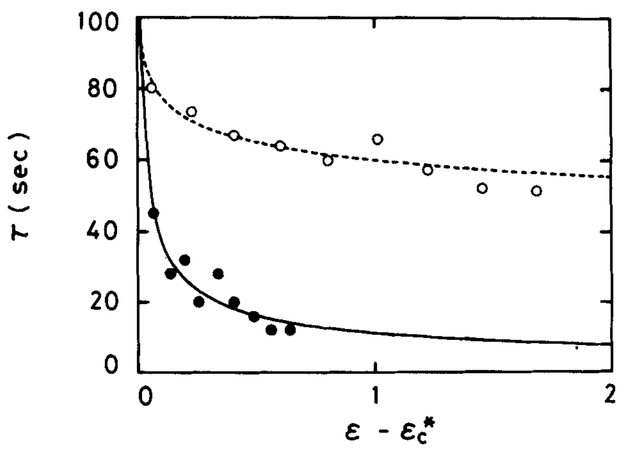

FIGURE 3 ε dependence of correlation time τ calculated from spatio-temporal maps. The symbols indicate the same as in Figure 2.

of a sample cell, ξ the correlation length in the x-direction and the correlation time τ is given in a unit of second. The indeces, which are usually related to fractality of patterns, show large difference due to Γ. One obtains a typical propagating velocity of fluctuations $v_{g1} = d\xi_{10}/\tau_{10} = 0.017d$ μm s^{-1} for $\Gamma = 15$ and $v_{g2} = 0.058d$ μm s^{-1} for $\Gamma = 650$. The higher the density of defects, the shorter the correlation length because of more random patterns. Similarly the larger the aspect ratio, the faster the gliding velocity and therefore the shorter the correlation time. In FWD, the major defect motion is the gliding rather than the climbing. Therefore v_g is closely related to the gliding velocity of defects. We learn from the ε dependence of defect density that ξ for, a deviation from the threshold of FWD, $\Delta\varepsilon$ $(=\varepsilon - \varepsilon_c^*) < 0.28$ in $\Gamma = 650$ is larger than that in $\Gamma = 15$ whereas this relation is inversed for $\varepsilon - \varepsilon_c^* > 0.28$ (compare a result in Figure 5). The minimum correlation length ξ_{min} is approximately equal to the thickness d of a cell. The maximum defect density therefore corresponds to $1/\xi_{min}$. Sharp decrease and small value of τ in $\Gamma = 650$ express more random motion than in $\Gamma = 15$.

Figure 4 indicates temporal change of defect numbers, probability distribution and a series of power spectra from the above in various ε for $\Gamma = 650$. Each power spectum is obtained by the average of ten measurements. With increase of ε, as already reported, discreteness of defect change is less pronounced and its temporal change looks more nonperiodic. For low ε in the cell of $\Gamma = 15$, the even number state of defects is more favourable than the odd. In the high density, *e.g.* for ε =

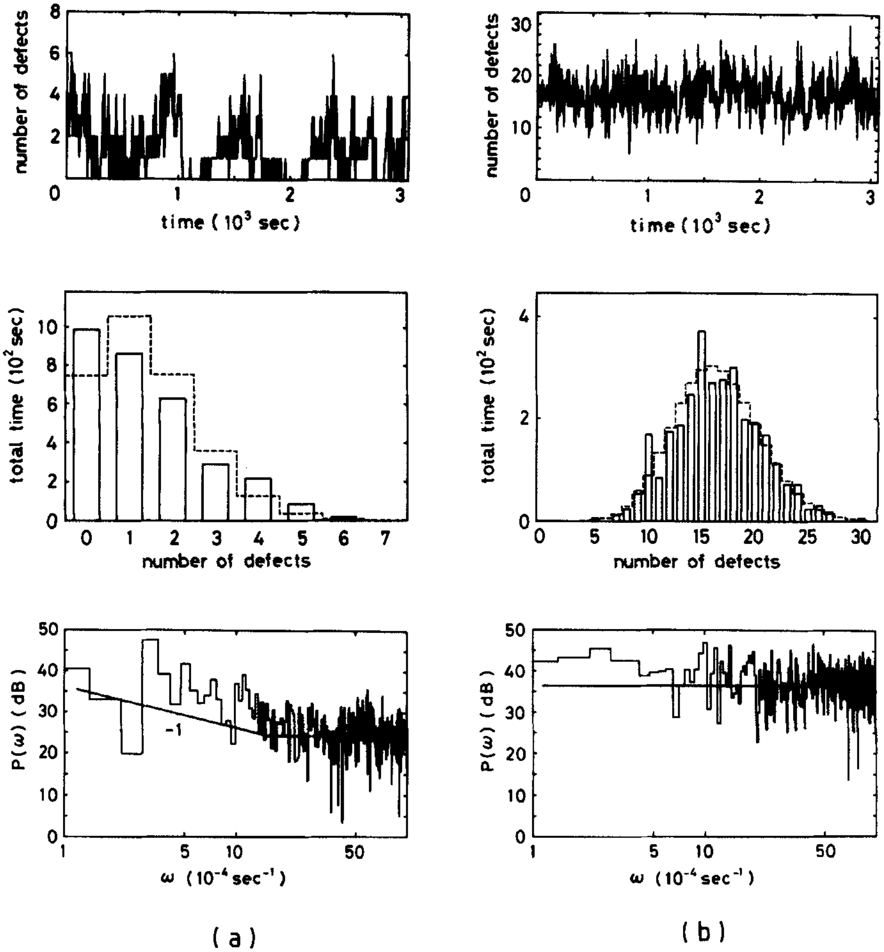

FIGURE 4 Temporal change of defect number (top figure), probability distribution of defects (middle figure) and power spectrum (bottom figure) ($\Gamma = 650$, sample No. 2). The dotted line in the middle figure shows conventional Poisson distribution. (a) $\Delta\varepsilon = 0.14$, (b) 0.49.

1.23 ($\Delta\varepsilon$ = 0.80), however, the even and odd number of defects can be observed with equal possibility. For Γ = 650, this does not happen because of high density.

We tried to fit the distribution with both conventional Poisson and square Poisson. It is however difficult to say which one is better for low density of defects but at least for high density of defects Poisson distribution gives rather better fitting. No better-fitness with square Poisson in high density case will be understandable from the fact that square Poisson is obtained under the assumption of noncorrelated pair-nucleation "far from" existing defects. In high density case this assumption does not hold. Nevertheless in low density of defects where it would be the case both Poisson and square Poisson do not well fit enough in the present experiment. Therefore we did not show the theoretical curves for the square distribution. Instead well-fitted Poisson cases for large Γ is shown in Figure 4. The reason is unknown yet.

In the cell of Γ = 15, a power spectrum shows basically $1/f$ type profile for almost all values of ε in FWD because of low density of defects.[5] On the other hand, in the cell of Γ = 650, a power spectrum shows $1/f$ type when $\Delta\varepsilon < 0.28$ where rather defect density is lower, but white when $\Delta\varepsilon > 0.28$ where defect density is high and almost reaching to the minimum distance allowing two neighboring defects. The profile change from $1/f$ to white in Γ = 650 appears to be gradually enhancing the amplitude of high frequency modes as long as looking at the power spectrum (see Figure 4).

According to our visual observation the density of defects is higher near edges of lateral boundary and lower in the center of a cell. This shows that the lateral boundary can influence the formation of defects. For small Γ, however, annihilation of defects to lateral boundaries is difficult to occur and mainly nucleation and annihilation of pairs occur in bulk. This is different aspect from defect motions in WD.[5]

All results in the present investigation would be summarized in Figure 5 which show the ε dependence of mean defect number obtained from the probability distributions of defects for two largely different aspect ratio. A mean defect density is normalized by d^2. At ε larger than $\Delta\varepsilon \sim 0.28$ the mean defect density is approx-

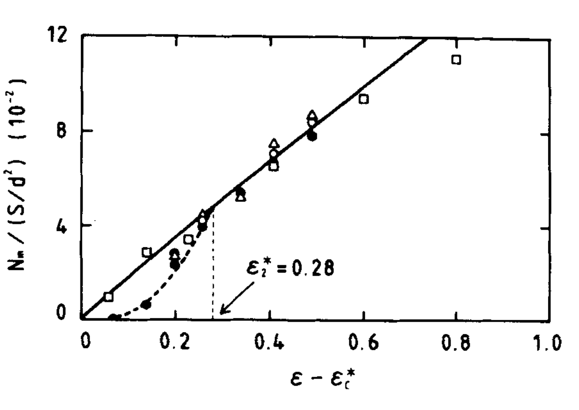

FIGURE 5 ε dependence of mean defect density for two Γs and four different cells. ○, △, □: Γ = 15 and ●: Γ = 650. ε_2^* is the cross-over point. The solid line is linear and the dotted line indicates $\Delta\varepsilon^2$. S is the observation area.

imately proportional to ε independently of Γ. But at smaller than that value, it depends on Γ, *i.e.* proportional to $\Delta\varepsilon^{0.95\pm0.08}$ for $\Gamma = 15$ and asymptotically exponentially[9] proportional to $\Delta\varepsilon$ or proportional to $\Delta\varepsilon^{2.0\pm0.3}$ for $\Gamma = 650$. Because of high density of defects for $\Delta\varepsilon > 0.28$, interactions among defects cannot be neglected and their dynamics is obviously influenced each other and changed. Such a interaction might give the linear ε dependence. On the one hand, there is no interaction among defects for $\Gamma = 650$ in the case of sufficiently low density of defects and far from lateral boundaries which is only possible for large Γ, and it needs not to consider image forces. The dynamics therefore must be different from previous case and gives the nonlinear ε dependence. This would be a reason why two different dependences come out for $\Gamma = 650$.

3. SUMMARY

The spatio-temporal patterns show different features depending on a aspect ratio. In small Γ strong collective motion of defects can be observed. The obtained distribution does not fit with either conventional Poisson or square Poisson. The experimental error deciding how clear defect should be counted would be larger. Two different power spectra, *i.e.* $1/f$ and white type, are observed in temporal change of defect number, which depends on defect density. $1/f$ spectrum can be observed in rather low density regime, and originates from the boundary effects and discreteness of temporal change of defect numbers. However the most important result obtained in the present study is the ε dependence of mean defect number which shows clear slope change. This cross-over of the ε dependence suggests a change of kinetics of formation and annihilation of defects due to correlation length and therefore two different states or a kind of critical phenomena for defect-mediated turbulence (FWD).

References

1. S. Kai and K. Hirakawa, *Mol. Cryst. Liq. Cryst.*, **40**, 261 (1977).
2. S. Kai and K. Hirakawa, *Prog. Theor. Pys.*, supp. **64**, 212 (1978).
3. X. D. Yang, A. Joet and R. Ribotta, Propagation in Systems far from Equilibrium, edited by J. E. Wesfreid and S. Zaleski (Springer-Verlag, Berlin, 1984).
4. I. Rehberg, S. Rasenat and V. Steinberg, *Phys. Rev. Lett.*, **62**, 756 (1989).
5. S. Kai, M. Kohno and N. Chizumi, *J. Phys. Soc. Jpn.*, **58**, 1493 (1989); *J. Phys. Soc. Jpn.*, **58**, 3541 (1989); *Phys. Rev.*, A**40**, 6554 (1989).
6. P. Coullet, L. Gill and J. Lega, *Phys. Rev. Lett.*, **62**, 756 (1989).
7. L. Gil, J. Lega and J. L. Meunier, *Phys. Rev.*, A**41**, 1138 (1990).
8. S. Kai and W. Zimmermann, *Prog. Theor. Phys.*, supp. **99**, 458 (1989).
9. M. Sano, S. Nasuno and Y. Sawada, private communication.
10. M. Kaiser, W. Pesch and E. Bondenschatz, private communication (1990).